J. Condensed Matter Nucl. Sci. 1 (2007) 106–128

Research Article

Fusion Rates of Bosonized Condensates*

Akito Takahashi†
High Scientific Research Laboratory, Marunouchi 24-16, Tsu, Mie 514-0033, Japan and Osaka University, Yamadaoka 2-1, Suita, Osaka 5650871, Japan

Norio Yabuuchi
High Scientific Research Laboratory, Marunouchi 24-16, Tsu, Mie 514-0033, Japan

Abstract

In Section 1, theoretical basis for formulating fusion rates in condensed matter is summarized. Nuclear strong interaction, S-matrix, T-matrix, fusion rate for steady state dde* molecule as bosonized condensate, and fusion rate formula for collision process are briefly given. In Section 2, application for TSC-induced fusion is summarized. Fusion rate formulas for adiabatic approach in EQPET theory are summarized. Final state interaction is briefly discussed. Time-dependent approach for TSC squeezing motion is briefly introduced.

Keywords: Bosonized condensate, dde* molecule, EQPET, Fusion rate formula, Time-dependence, TSC-induced reaction

1. Basic Theory

1.1. Nuclear Potential

In general, nuclear reaction is usually theorized and analyzed in three steps; initial state interaction, intermediate compound state, and final state interaction. Transition from intermediate state to final state has various, sometimes complex, channels such as the electro-magnetic transition to ground state emitting gamma rays, the particle (neutron, proton, α-particle, etc.) emission and residual nucleus, which sometimes decay to ground state emitting gamma-rays, and the direct break-up to two or more nuclei like fission. Potential for nuclear strong force and Coulomb force in these cases can be categorized into three cases [1] of Fig. 1.

The potential state (I) shows the case that nucleons (neutrons and protons) are trapped in a very deep well of strong force. Stable isotopes of masses less than 60 have this type potential well. Fusion reactions by two light nuclei produce stable isotopes of this type.

*Submittal to the 7th International Workshop on Anomalies in Hydrogen/Deuterium Loaded Metals, September 2006.
†E-mail: akito@sutv.zaq.ne.jp

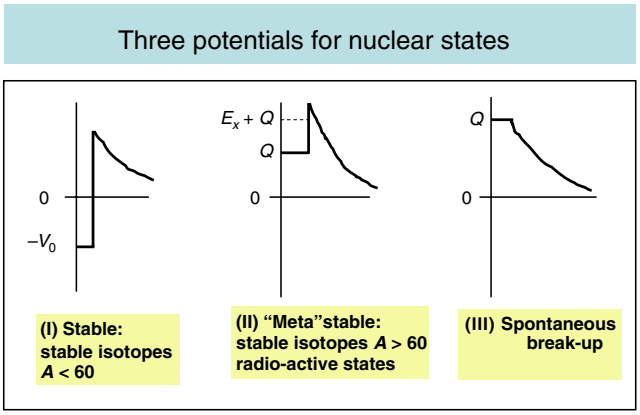

Figure 1. Three potential types for nuclear interaction.

The potential state (II) appears for intermediate compound state in general. Radioactive isotope has this kind of potential. Stable isotopes having masses greater than 60 are trapped in these type potentials, which are drawn according to the fission channels breaking-up to lighter nuclei. In this case, the depth of trapping potential is deep enough to have very long lifetime, but positive Q-value for fission channels makes height of potential tail in outer-skirt lower than the depth of trapping well. At ground state, the thickness of potential well is large enough to make the quantum-mechanical tunneling probability of fission to be "inverse-astronomically" very close to zero.

Therefore, nucleus is regarded as stable isotope. Here, Q-value is obtained by calculating mass defect between before and after reaction, using Einstein's formula $E = mc^2$. However, when the intermediate compound nucleus has high inner excited energy E_x, the thickness of outer wall of trapping potential becomes relatively thin and quantum mechanical tunneling probability for particle emission or fission can dramatically increase. Fission process for uranium and trans-uranium nuclei is induced in this way. Moreover, we may have possibility of fission for lighter nuclei with mass $A < 200$. In some of proposed theories [2–4] in the Condensed Matter Nuclear Science (CMNS), deterministic models of fission for $60 < A < 200$ nuclei have been developed.

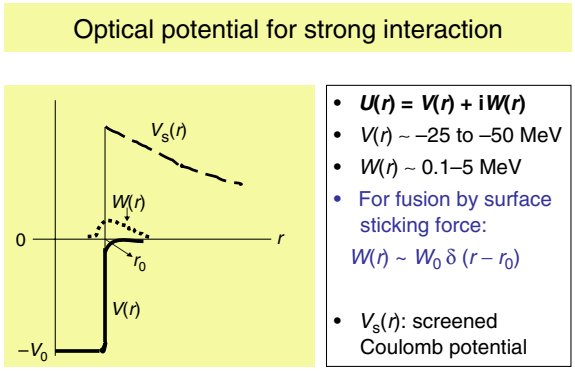

Figure 2. Optical potential for strong interaction.

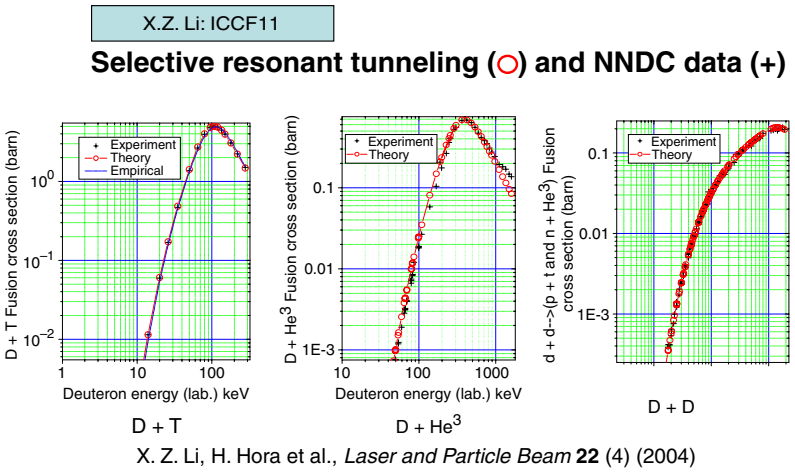

Figure 3. Fusion cross-sections for dt, d^3He and dd processes.

The potential type (III) is the case for intermediate compound nucleus having very high inner excited energy Ex, such as cases of fusion reactions of hydrogen isotopes. Compound nucleus in this case promptly breaks up to fragment-particles.

1.2. Strong Interaction

Now we explain very briefly the feature of potential by nuclear strong interaction. The reason why nucleons are trapped within very small spherical space with radius about 5 fm (1 fm $=$ 10^{-15} m) was first solved by the famous Yukawa model of pion exchange. Hideki Yukawa won Nobel Prize by this theory. Later, the theory of strong force has been deepened by the development of QCD [5] based on concept of quark and gluon. However, as the conclusion in recent views of nuclear physics, the strong interaction can be drawn accurately enough by the Yukawa model with charged pions (π^+, π^-) and neutral pion, for relative reaction energy less than about 200 MeV (less than the threshold energy of pion-generation). Especially, for fusion reaction process, charged pions play role of sticking two (or more) nuclei.

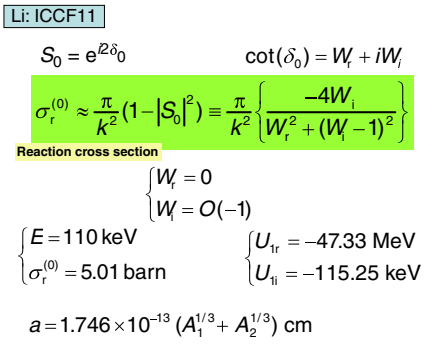

Figure 4. Fitting of dt fusion cross-sections by *S*-matrix formulas by Li et al. [9].

Nuclear fusion by strong interaction can be simulated by the catch-ball model of charged pions between nuclei for fusing. Due to the very short range of de Broglie wave length (about 2 fm) of pion, the strong interaction for fusion becomes very short range force, namely "almost on surface" sticking force. For example, when relatively large ($A > 6$) two nuclei approach closely, fusion force by exchanging charged pions (between neutron and proton for counter-part nuclei) becomes the sticking force near at surface ($R = r_0$). Exchange of neutral pion for scattering (repulsive) force between nucleons of counter-part nuclei also happens in the region relatively near at surface.

Especially, nuclear fusion reactions at very low energy as cold cluster fusion and transmutation as modeled by EQPET/TSC theory (see Section 2), largeness of surface area for exchanging charged pions governs the largeness of reaction cross-section. This is specific character of "nuclear reactions in condensed matter".

1.3. Optical Potential

Global optical potential [6], written by complex number, is used for nuclear potential of strong interaction for scattering and sticking forces. Image of global optical potential is drawn in Fig. 2. The real part, namely deep trapping potential $V(r)$ is a well with rather round shape near at surface of nucleus (Woods–Saxon type), but is approximated to be constant value V_0 within in nucleus.

$$U(r) = V(r) + iW(r). \tag{1}$$

V_0 is about -25 MeV for deuteron. V_0 value saturates to about -50 MeV for nuclei of $A > 24$.

Imaginary part $W(r)$ corresponds to the interaction of charged-pion exchange, and locates near at surface ($r = r_0$) to be approximated by delta-function $W_0\delta(r - r_0)$. When we use this delta-function approximation, fusion rate formula becomes simple.

1.4. T-matrix and Reaction Cross-section

Now we briefly summarize quantum mechanical basis of scattering and reaction process.

Asymptotic wave function [6,7] after scattering (interaction) is written by Eq. (2).

$$\Psi(r) \approx \mathrm{e}^{ikz} + f(\theta)(\mathrm{e}^{ikr}/r). \tag{2}$$

Differential cross-section of process is defined by

$$\frac{\mathrm{d}\sigma}{\mathrm{d}\Omega} = |f(\theta)|^2. \tag{3}$$

S-matrix is defined by the phase-shift analysis [6,7] as using Legendre polynomial expansion for scattering amplitude $f(\theta)$,

$$f(\theta) = (1/2ik)\sum_{l=0}^{\infty}(2l+1)(S_l - 1)P_l(\cos\theta), \tag{4}$$

$$S_l = \mathrm{e}^{2i\delta_l}. \tag{5}$$

In general reaction process, not only elastic scattering but also absorption, fusion, particle emission processes are taking place as transition. To treat the transition from (α, β) to (α', β') channel, evaluation of T-matrix elements are usually done. T-matrix is defined [7] by the following Lippmann–Schwinger equation,

$$T = U + UG_0T, \tag{6}$$

$$G_0 = (E - H_0 + i\delta)^{-1}, \tag{7}$$

$$H = U + H_0. \tag{8}$$

Here, G_0 is the Green operator for H_0 Hamiltonian with kinetic energy and spin Hamiltonian only. So, U is regarded as the effective interaction Hamiltonian.

Scattering amplitude is defined by,

$$f(\theta; \alpha\beta \to \alpha'\beta') = -(2\pi/h^2)\left\langle \Psi_{\alpha'\beta'}|T|\Psi_{\alpha\beta}\right\rangle. \tag{9}$$

If we approximate $T = T^{(0)} = U$, formula (9) becomes the Born approximation.

Lippmann–Schwinger equation can be regarded as an integral type equation of Schroedinger differential equation. The first-order approximation of T is given by inserting $T = U$ in Eq. (6), and we get $T^{(1)} = U + UG_0U$. The second-order approximation is then given as $T^{(2)} = U + UG_0T^{(1)}$, and the nth order approximation gives $T^{(n)} = U + UG_0T^{(n-1)}$. This successive treatment is known as Neumann series solution [8] of integral equation.

We can treat reaction cross-section including transition by evaluating T-matrix elements.

For the optical potential of $V + iW$ type with constant V and W values, formulas of reaction cross-section are given in standard text book of nuclear physics (Chapter 9 of Ref. [6], for example) for S-wave ($l = 0$).

$$\sigma_{r,0} = \pi\bar{\lambda}^2 \frac{-4kR\,\mathrm{Im}\,f_0}{(\mathrm{Re}\,f_0)^2 + (\mathrm{Im}\,f_0 - kR)^2}, \tag{10}$$

$$K = \frac{1}{\hbar}\sqrt{2M(E + V + iW)}, \tag{11}$$

$$f_0 = KR\ \cot\ KR. \tag{12}$$

And relations between S-matrix and T-matrix for Legendre coefficients are:

$$T_\ell = \mathrm{e}^{i\delta_\ell}\ \sin\ \delta_\ell, \tag{13}$$

$$S\ell = 1 + 2iT_\ell. \tag{14}$$

By evaluating T-matrix elements, we can treat reaction with channel transition.

As shown in Figs. 3 and 4, Li evaluated [9] fusion cross-section for dd, dt and d^{3}He reactions using S-matrix formulas. Fusion cross-sections are shown in Fig. 3. S-matrix formula and evaluated values of V and W (written as U_{1r} and U_{1i} in Fig. 4) for dt reaction are shown in Fig. 4.

Li used the reaction cross-section formula with S-matrix elements as shown in Fig. 4. He obtained averaged values of V and W of optical potential by fitting calculated curves to experimental cross-sections.

As explained in nuclear physics text books [6], S-matrix elements by the phase-shift analysis can be used for estimating not only elastic scattering cross-section but also total reaction cross-section. However, the phase-shift analysis does not give information on out-going channels and products by final state interaction.

1.5. Imaginary Part of Optical Potential

Now we move to the explanation of physical meaning for the imaginary part W of optical potential. From the conservation of quantum mechanical probabilistic density flow (a kind of continuity equation), we can take meaning of the imaginary part.

The forward Schroedinger equation is

$$i\hbar\frac{\partial\Psi}{\partial t} = \left[-\frac{\hbar^2}{2M}\nabla^2 + V + iW\right]\Psi \tag{15}$$

and the backward or adjoint equation is

$$-i\hbar\frac{\partial\Psi^*}{\partial t}=\left[-\frac{\hbar^2}{2M}\nabla^2+V-iW\right]\Psi^*. \tag{16}$$

Here we used complex conjugate potential for the adjoint (backward) equation.

We multiply Ψ^* on Eq. (15) from the left side, multiply Ψ on Eq. (16) from the left side and make mutual subtraction to get for the left hand side:

$$i\hbar\left(\Psi^*\frac{\partial\Psi}{\partial t}+\Psi\frac{\partial\Psi^*}{\partial t}\right)=i\hbar\frac{\partial\Psi\Psi^*}{\partial t}=i\hbar\frac{\partial\rho}{\partial t}. \tag{17}$$

Here,

$$\rho=\Psi\Psi^*. \tag{18}$$

And we get for the right hand side:

$$i\hbar\frac{\partial\rho}{\partial t}=-\frac{\hbar^2}{2M}\left[\Psi^*\nabla^2\Psi-\Psi\nabla^2\Psi^*\right]+i\left[2W\rho\right]=-i\hbar\,\mathrm{div}\,\vec{j}+i\left[2W\rho\right]. \tag{19}$$

Here we used formulas of quantum mechanical current flow as

$$\begin{aligned}\vec{j}&=\frac{\hbar}{2im}(\Psi^*\vec{\nabla}\Psi+\Psi\vec{\nabla}^*\Psi^*)\\&=\frac{\hbar}{2im}(\Psi^*\vec{\nabla}\Psi-\Psi\vec{\nabla}\Psi^*),\end{aligned} \tag{20}$$

$$\begin{aligned}\mathrm{div}\,\vec{j}&=\frac{\hbar}{2im}(\vec{\nabla}(\Psi^*\vec{\nabla}\Psi)-\vec{\nabla}((\Psi\vec{\nabla}\Psi^*))\\&=\frac{\hbar}{2im}(\Psi^*\nabla^2\Psi+(\vec{\nabla}\Psi^*)(\vec{\nabla}\Psi)-\Psi\nabla^2\Psi^*-(\vec{\nabla}\Psi)(\vec{\nabla}\Psi^*))\\&=\frac{\hbar}{2im}(\Psi^*\nabla^2\Psi-\Psi\nabla^2\Psi^*).\end{aligned} \tag{21}$$

Consequently, we obtain the modified continuity equation for probabilistic density flow:

$$\frac{\partial\rho}{\partial t}=-\mathrm{div}(\vec{j})+\frac{2}{\hbar}W\rho. \tag{22}$$

It is obvious that the second term of Eq. (22) corresponds to the absorption rate term of the balance. (We do not have the second term in the continuity equation of fluid.)

Mean-free-path of particle in the strong force field of optical potential is given as (velocity) × (lifetime), namely:

$$\Lambda=(\hbar/2)v/W(r). \tag{23}$$

1.6. Fusion Rate for Steady Molecule

We now move to formulate fusion rate formulas for pseudo-molecule (EQPET molecule) [10–19] of two deuterons and bosonized electrons (quasi-particle) $e^*(m/m_e, Z)$. Here, m_e is the electron mass and Z is number charge of quasi-particle.

For deriving the trapping Coulomb potential, we will treat it later. Here, we assume an EQPET molecule is trapped in a shielded Coulomb potential similar to the Morse potential [8]. We illustrate the image of shielded Coulomb potential $V_s(r)$ with optical potential in Fig. 5. Scales are deformed for easy understanding the feature.

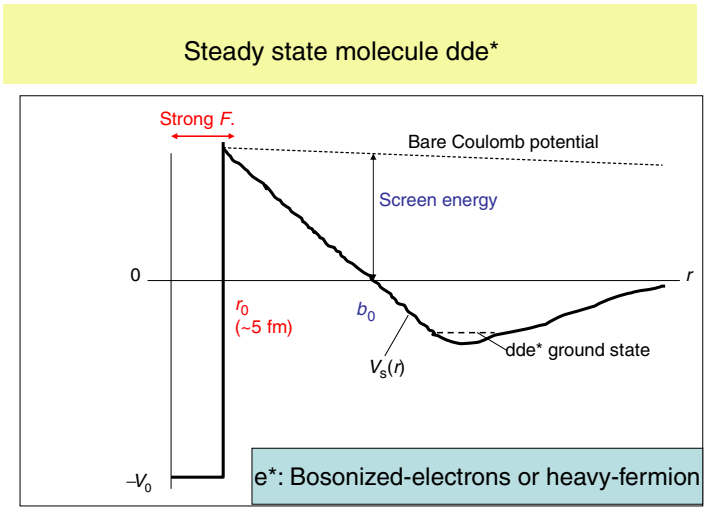

Figure 5. Trapping Coulomb+strong force potential for steady EQPET molecule of dde*.

Range of strong nuclear force is very short in several fm regions, and concentrated in near surface ($r = r_0$) of nucleus. On the other hand, Coulomb interaction as electro-magnetic force distributes from r_0 to nm long region effectively.

As a result, fusion rate for low energy under the strong interaction at around $r = r_0$ can be treated by adiabatic

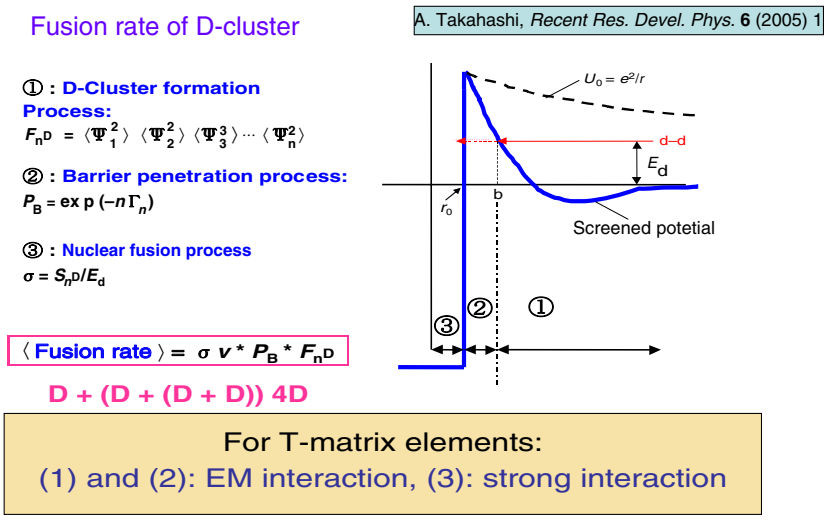

Figure 6. Three adiabatic steps for formulating fusion rate in condensed matter.

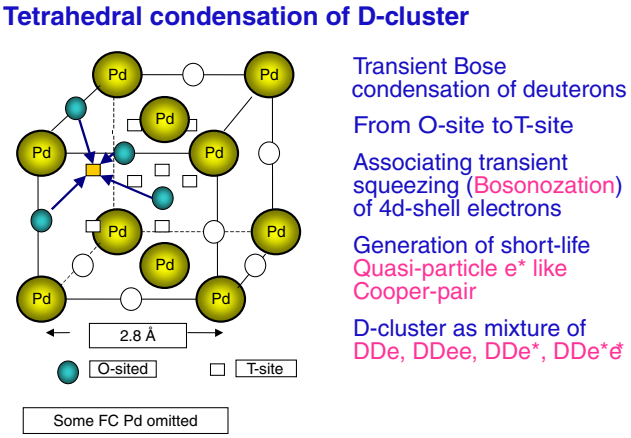

Figure 7. Model-A for TSC formation in PdD lattice under D-phonon excitation.

approximation (namely Born–Oppenheimer approximation in quantum mechanics) to take product of the absorption rate by nuclear optical potential (imaginary part) and the tunneling probability of dd pair at $r = r_0$.

Fusion rate per dd pair is therefore defined as

$$\lambda_{\mathrm{dd}} = T_{\mathrm{n}} |\Psi(r_0)|^2, \tag{24}$$

$$T_{\mathrm{n}} = (2/\hbar)\, \langle \Psi_{\mathrm{f}} | W(r) | \Psi_i \rangle\,. \tag{25}$$

Here, $|\Psi(r_0)|^2$ is equivalent to the quantum mechanical tunneling probability of dd pair through the shielded Coulomb potential $V_{\mathrm{s}}(r)$, as given by the WKB approximation [7]. Fusion rate for muonic molecule dde*(208,1) can be approximately given by Eq. (24), assuming the lifetime of muon is long enough. Actually the lifetime of muon is 2.2 μs, and trapping potential should be regarded as adiabatic.

1.7. Fusion Rate for Dynamic Process

For more transient and dynamic process than muonic dd molecule, it is better to use formulas (Fermi's second golden rule) for cross-section. Especially, for fusion rate calculations of EQPET molecules dde*(2,2), dde*(4,4), dde*(6,6), dde*(8,8), lifetimes of pseudo-molecules are much shorter (assuming on the order of femto-second) than muonic dd molecule.

Fusion rate is formulated as

$$\lambda = \sigma v = (1/\hbar) v T^2 \rho(E'), \tag{26}$$

$$T = \langle \Psi_{\mathrm{f}} | H_{\mathrm{int}} | \Psi_i \rangle\,. \tag{27}$$

Here v is the relative velocity for d–d interaction, $\rho(E')$ is the final state density, and H_{int} is the effective interaction Hamiltonian as given by the approximate solution of Lippmann–Schwinger equation.

Fusion rate per dd pair is given by $\langle \sigma v \rangle$. Cross-section σ is proportional to the square of T-matrix. To evaluate T-matrix elements, we need to treat many steps of physics as the formation process of EQPET dde* molecule by the consequence of electromagnetic interaction in ordered (or constrained) space in condensed matter—solid state

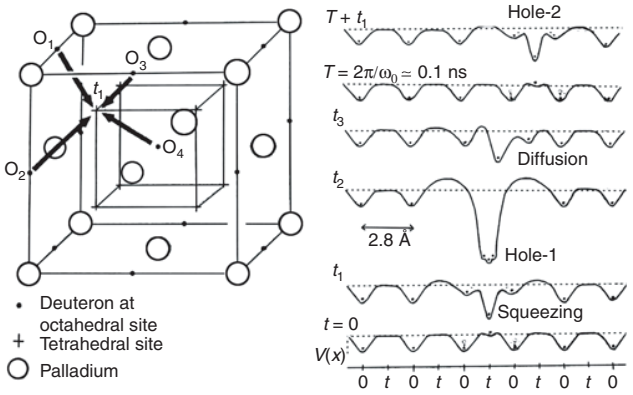

Figure 8. Image of lattice potential change by D-phonon excitation.

physics calculation of dynamic behavior of deuterons in lattice Bloch potential, atomic physics calculation to evaluate shielded Coulomb potential $V_s(r)$ and strong interactions by global optical potential. After that, we need to evaluate the intermediate compound state with excited energy and spin-party state. Finally, we have to evaluate out-going channels and branching ratios of the final state interaction. In every step, we need to evaluate T-matrix elements.

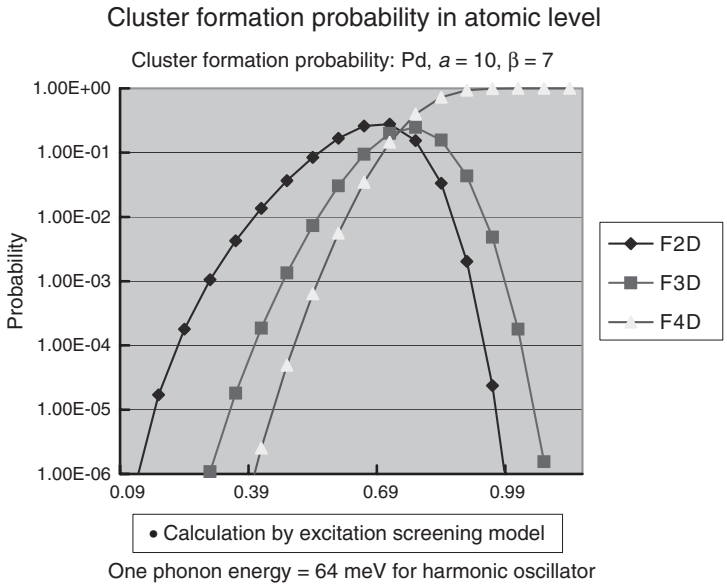

Figure 9. Example of estimation of D-cluster formation probability [20].

2. Example: EQPET/TSC Model

2.1. Tetrahedral Symmetric Condensate (TSC)

As a seed of cold fusion or more extendedly condensed matter nuclear effects, a charge-neutral entity (pseudo-particle) of Platonic regular polyhedron composed with alternative positioning of deuteron (or proton) and electron at vertex of polyhedron has been porposed [9–19]. A representative one is the tetrahedral symmetric condensate (TSC), which is composed of four deuterons forming a regular tetrahedron and four electron balls also forming a regular tetrahedron. Each particle or ball sits at vertexes of cube. An electron ball at vertex depicts effective electron center of coupled two electrons having opposite spins each other. TSC is a transient pseudo-particle with short life (on the order of 100 fs at shortest). Exact place and condition for TSC production is still open question, but two models were proposed [11–17]. One (Model A) is the transient formation of TSC at T-sites of PdD under D-phonon excitation. The other (Model B) is the resonant coupling of two D_2 molecules at some focal points (corner hole, defect, etc.) in near surface of metal-deuteride. TSC can make time-dependent squeezing motion under three-dimensional constraint to condensate at central focal point to become transiently a very small (on the order of 10 fm) charge-neutral pseudo-particle, which will make self-fusion of four deuterons within strong interaction (charged-pion exchange) range or will make deuteron-cluster-capture reaction with host metal nucleus [11–17].

Estimation of fusion rate by the TSC squeezing motion has been formulated by evaluating T-matrix elements in three adiabatic steps, as illustrated in Fig. 6.

The first adiabatic process is for estimating D-cluster formation probability in condensed matter.

$$F_{\mathrm{nd}} = \left\langle {\Psi_1}^2 \right\rangle \left\langle {\Psi_2}^2 \right\rangle \left\langle {\Psi_3}^2 \right\rangle \left\langle {\Psi_4}^2 \right\rangle \cdots \left\langle {\Psi_n}^2 \right\rangle, \tag{28}$$

where Ψ_n is the "lattice" wave function for the nth deuteron. To estimate the D-cluster formation probability F_{nd} is most important for predicting experimental conditions. However practical modeling is of open question for future research.

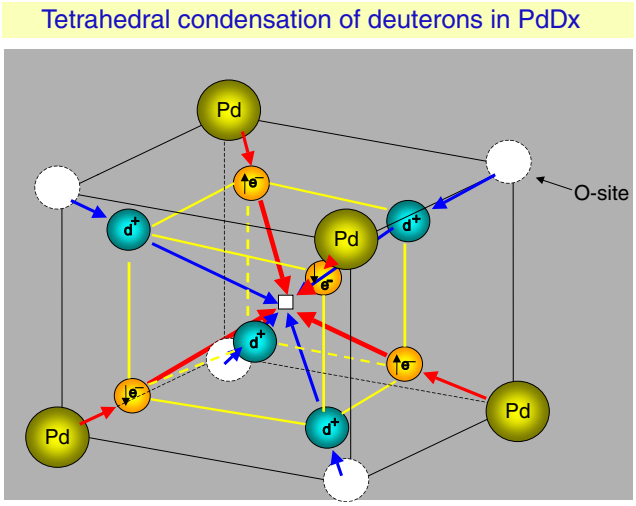

Figure 10. Image of TSC formation in PdD lattice under statistical coherence by phonon excitation.

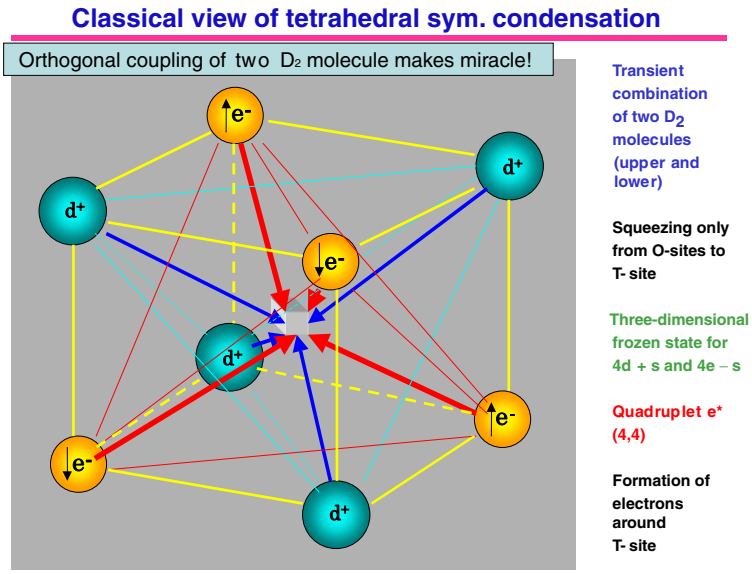

Figure 11. Semi-classical view of TSC (tetrahedral symmetric condensate) for four deuterons and four electron-balls (here electron balls are drawn as single electrons).

The second adiabatic process is for estimating quantum mechanical barrier penetration probability P_B. P_B is approximately given by the WKB method [7] as

$$P_B = \exp(-n\Gamma_n), \tag{29}$$

where Γ_n is Gamow integral for n-deuterons cluster and given as,

$$\Gamma_n = (\sqrt{2\mu}/h)\int_{r_0}^{b}\sqrt{V_s(r) - E_d}\,dr. \tag{30}$$

Here μ is the reduced mass and r_0 and b are given in Fig. 5. For very low energy fusion reaction, b is approximately given by b_0. Once the adiabatic screened potential, as illustrated in Fig. 5, is calculated, for example as we show later by the EQPET model [11–19], the Gamow integral can be numerically obtained by Eq. (30). The barrier penetration probability for multi-body fusion process is given in Eq. (29) by assuming that multi-body interaction takes place as very rapid cascade process of two-body interactions.

The third adiabatic process is for estimating cross-section of multi-body strong interaction. Instead of evaluating T-matrix directly, it is more practical to use S-value, the astrophysical S-value, to write fusion cross-section by strong interaction only as,

$$\sigma_{strong} = S_{nd}/E_d. \tag{31}$$

Pure theoretical estimation of S-values for multi-body interaction is difficult because of so many-body (exchanging more than six charged pions for 3d, 4d, 6d, and 8d fusion) problems. We introduce instead an empirical extrapolation as shown later.

Model A for TSC formation is illustrated in Fig. 7. We assume local fulfillment of $x = 1$ for PdDx lattice. We do not necessarily require the $x = 1$ condition (full D-loading) for balk Pd sample. The local $x = 1$ condition may

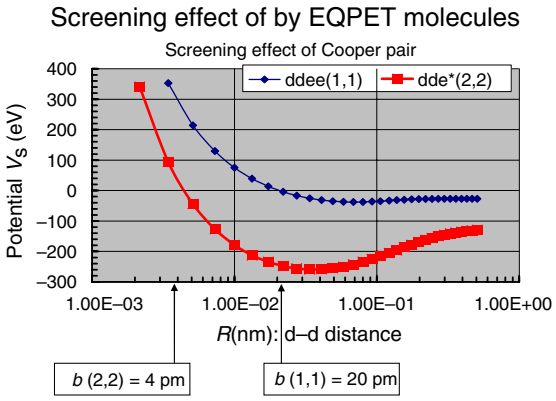

Figure 12. Screened Coulomb potential for ddee (D_2 molecule) and dde*(2,2) (EQPET molecule with Cooper pair); change of b-parameter with deepening of negative potential depths results in condensing force for dde* pseudo-molecule.

be fulfilled in near surface zone of Pd sample in experiment. Then we assume that D-in lattice is excited to higher phonon energy state by external stimulation. Laser beam irradiation on Pd sample surface may be a stimulation method for optical phonon excitation. It is known that D in PdDx lattice sits as Harmonic oscillator with $\hbar\omega = 64$ meV and $E_0 = 32$ meV.

As a function of phonon energy, we can estimate D-cluster formation probabilities at central T-sites, as example of such calculation is shown in Fig. 9. However this process is essentially time-dependent (transient), and we have to treat more exactly the process as illustrated in Fig. 8. We may first estimate the D-cluster formation probability within a small time-interval of "deep trapping hole" in Fig. 8, by treating adiabatically the state (adiabatic dde* state). Then we will make time-averaging for the periodical oscillation process. The adiabatic dde* state is regarded as the most squeezed state (MSS). Numerical calculation for screened potential $V_s(r)$ will be then done (shown later) by EQPET.

The example of D-cluster formation probability for Model A, as shown in Fig. 9, is the treatment [20] with quantum mechanical statistics, which does not include anti-parallel spin configuration for pairing electrons forming electron balls, neither treating the three dimensional constraint of squeezing motion under Platonic symmetry yet.

Centralized point-symmetric coherence of momentum-vectors for four deuterons and four-electron balls is required to form TSC. This condition cannot be expected in random motion of particles in plasma. The squeezing motion under three-dimensional constraint (or ordering, or self-organization process) in lattice dynamics can realize that condition.

The semi-classical image of 4D cluster (TSC) is shown in Fig. 10. Pd atom has 10 outer most electrons in 4d-shell. Pd atom is unique atom having largest number of valence electrons among atoms in nature. Electrons in 4d-shell contribute as quasi-free conduction-band electrons in Pd metal lattice.

Transition of physical system happens to realize the system-energy minimum state. The local energy minimum condition is formulated by the variational principle of quantum mechanics [7,8]. Eigen-value problem is led to solve secular equation.

However, under the ordering process (or self-organization process) in three-dimensional constrained motion, the Platonic symmetry (regular polyhedron) for alternative positioning of deuteron (proton) and electron-ball makes obviously the averaged system electric charge zero. Namely TSC realizes minimum system Coulomb energy. Hence the TSC state can be a particular solution of variational method.

The semi-classical image of TSC is shown in Fig. 11. Pair of counter-part two electrons is the combination of anti-parallel spins, combination probability of which can be estimated simply. When momentum vectors of pairing two

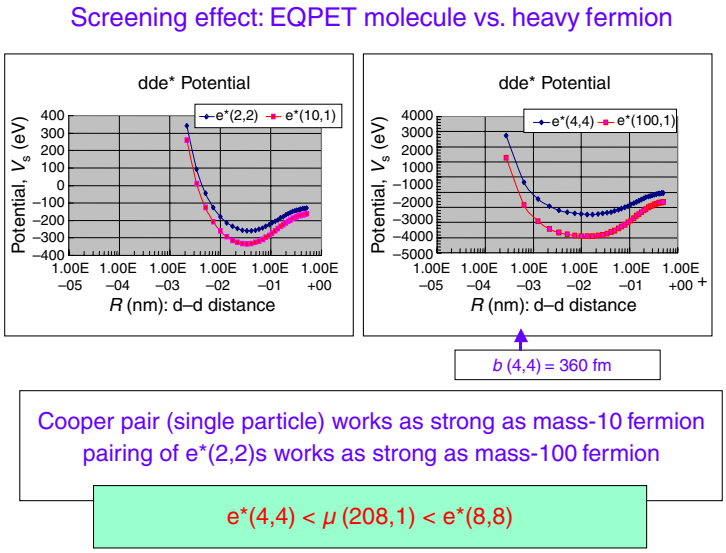

Figure 13. Comparison of screened Coulomb potentials between EQPET molecules and virtual molecules with heavy fermions; muon works as much as e*(6,6), cf. Tables 1 and 2.

electrons are 180° opposite configuration, the transient Cooper pair e*(2,2) is formed. Moreover, in TSC configuration, two Cooper pairs may couple orthogonally to form the quadruplet quasi-particle e*(4,4). As a general concept, this is the *bosonization* of electrons. Here, more exact quantum mechanical image for electron-ball is a pseudo-particle of 1/2 of coupling of two electrons with anti-parallel spin each other. More exact image is shown later in the time-dependent problem.

2.2. EQPET Model

It is difficult to evaluate directly the total TSC wave function because of so many-body problems. The EQPET (electronic quasi-particle expansion theory) model assumes that the total TSC wave function can be written by the

Table 1. Calculated screening energies by EQPET model

e*	U_s (eV)		b_0 (pm)	
	dde*	dde*e*	dde*	dde*e*
(1,1)	36	72	40	20
(2,2)	360	411	4	3.5
(4,4)	4000	1108	0.36	1.3
(8,8)	22,154	960	0.065	1.5
(208,1)	7579	7200	0.19	0.20
(6,6)	9600		0.15	

Screening energy of EQPET molecules $U_s = -e^2/b_0$ for $V_s(b_0) = 0$

linear combination of partial wave functions for EQPET molecules dde* for e*(2,2) and e*(4,4) and regular molecules dde ($D_2{}^+$ ion) and ddee (D_2 molecule).

$$|\Psi_N\rangle = a_1 \left|\Psi_{(1,1)}\right\rangle + a_2 \left|\Psi_{(2,2)}\right\rangle + a_4 \left|\Psi_{(4,4)}\right\rangle + a_6 \left|\Psi_{(6,6)}\right\rangle + a_8 \left|\Psi_{(8,8)}\right\rangle. \tag{32}$$

Here equation is written for including the case of OSC (octahedral symmetric condensate). For TSC, a_6 and a_8 are zero.

Fusion rate formula for dde* is given [11–19] by,

$$\lambda_{(i,j)} = v\,(S_{2\mathrm{d}}/E_{\mathrm{d}}) \exp\left(-2\Gamma_{(i,j)}\right), \tag{33}$$

$$\Gamma_{(i,j)} = 0.218 \int_{r_0}^{b(i,j)} \sqrt{V_{\mathrm{s}(i,j)}\,(R_{\mathrm{dd}}) - E_{\mathrm{d}}}\ \mathrm{d}R_{\mathrm{dd}}. \tag{34}$$

Here R_{dd} is the inter-nuclear distance between two deuterons in D-cluster.

The modal fusion rate for TSC system is given by

$$\lambda_N = {a_1}^2\lambda_{(1,1)} + {a_2}^2\lambda_{(2,2)} + {a_4}^2\lambda_{(4,4)} + {a_6}^2\lambda_{(6,6)} + {a_8}^2\lambda_{(8,8)}. \tag{35}$$

Formulas for screened Coulomb potentials V_{s} of EQPET molecules were given [11–19] by applying the solution for $D_2{}^+$ ion and D_2 molecule, based on the variational method [21], as for dde*,

$$V_{\mathrm{s}(i,j)} = \frac{e^2}{R_{\mathrm{dd}}} + V_{\mathrm{h}} + \frac{J+K}{1+\Delta}, \tag{36}$$

$$V_{\mathrm{h}} = -13.6(\mathrm{e}^*/\mathrm{e})^2 \left(m^*/m_{\mathrm{e}}\right). \tag{37}$$

Here V_{h} is the virtual binding energy of EQPET atom de*. And,

$$i = \mathrm{e}^*/\mathrm{e} \tag{38}$$

is the number charge of e*, and

$$j = m^*/m_{\mathrm{e}}. \tag{39}$$

The Coulomb integral J is given as

$$J = (Ze^2/a_{\mathrm{B}}) \left[-\frac{1}{y} + \left(1+\frac{1}{y}\right)\exp(-2y)\right]. \tag{40}$$

The electron exchange integral K is given by

$$K = (Ze^2/a_{\mathrm{B}})(1+y)\exp(-y). \tag{41}$$

Table 2. Main parameters of screened Coulomb potentials

Parameters of dde* potentials			
Trapping depth		Ground state	
e*(m, Z)	V_{smin}(eV)	b_0 (pm)	R_{dd} (gs) (pm)
(1,1)	− 15.4	40	101
(1,1) × 2; D_2	−37.8	20	73
(2,2)	−259.0	4	33.8
(4,4)	−2460	0.36	15.1

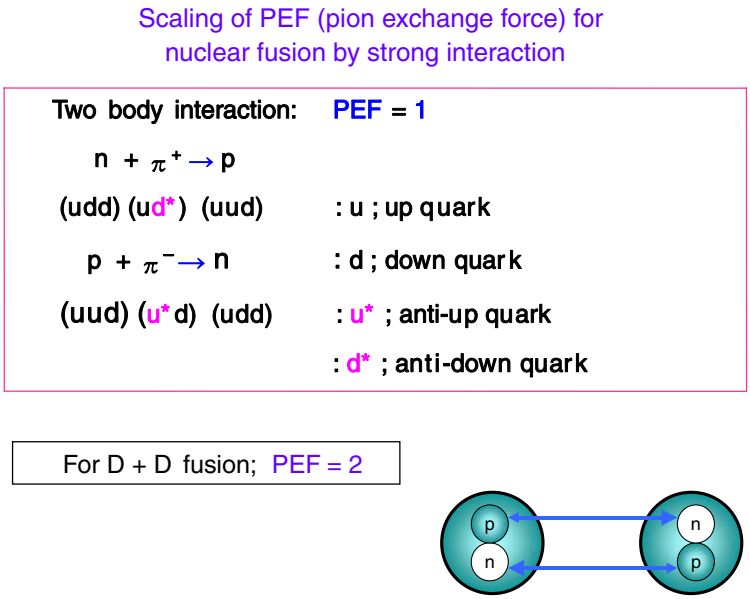

Figure 14. Definition of scaling measure PEF for fusion reaction.

The non-orthogonal integral is

$$\Delta = \left(1 + y + \frac{y^2}{3}\right) \exp(-y) \tag{42}$$

with

$$y = R_{\mathrm{dd}} / \left(a_{\mathrm{B}} / Z / \left(m^* / m_{\mathrm{e}}\right)\right). \tag{43}$$

Here $aB = a_{\mathrm{B}}/Z/(m^*/m_{\mathrm{e}})$, a_{B} is Bohr radius (52.9 pm) and $Z = \mathrm{e}^*/\mathrm{e} = i$.

Fusion rate for multi-body reaction is given approximately by

$$\lambda_{\mathrm{nd}(i,j)} = v\,(S_{\mathrm{nd}}/E_{\mathrm{d}}) \exp\left(-n\Gamma_{(i,j)}\right). \tag{44}$$

Modal fusion rate of multi-body fusion for TSC is then given by

$$\lambda_{N\mathrm{nd}} = \sum_i ai^2 \lambda_{\mathrm{nd}(i,j)}. \tag{45}$$

Calculated results of screened Coulomb potentials for EQPET molecules are shown in Figs. 12 and 13.

Compared to the bare Coulomb potential, a low energy d–d pair can come closer to the position b_0 classically and then penetrates quantum mechanically to the point $r = r_0$ of strong interaction range. It is well known that muonic molecule dde*(208,1) realize large dd fusion rate. Shielded Coulomb potential for dde*(4,4) is equivalent to the one for dde*(100,1), and dde*(6,6) has almost the same shielded Coulomb potential as muonic molecule. Here muon mass is used 207 plus 1 considering one electron added.

Screening energy by e* is estimated by calculating bare Coulomb energy at $r = b_0$. Calculated screening energies are given in Table 1.

Table 3. Calculated barrier factors and fusion rates (per cluster) for dde*

(m*,e*)	Barrier factor (BF)				Fusion rate (f/s/cl.) (FR)			
	2D	3D	4D	8D	2D	3D	4D	8D
(0,0)	10^{-1685}				10^{-1697}			
(1,1)	10^{-125}	10^{-187}	10^{-250}	10^{-500}	10^{-137}	10^{-193}	10^{-252}	10^{-499}
(2,1)	10^{-53}	10^{-80}	10^{-106}	10^{-212}	10^{-65}	10^{-86}	10^{-108}	10^{-211}
(2,2)	10^{-7}	10^{-11}	10^{-15}	10^{-30}	10^{-20}	10^{-17}	10^{-17}	10^{-29}
(4,4)	(3×10^{-4})	10^{-5}	10^{-7}	10^{-14}	(10^{-16})	10^{-11}	10^{-9}	10^{-13}
(8,8)	(4×10^{-1})	(2×10^{-1})	(1×10^{-1})	2×10^{-2}	(10^{-13})	(10^{-7})	(10^{-3})	10^{-1}

$E_d = 0.22$ eV and ( ) indicates that the value is virtual rate

2.3. Multi-Body Strong Interaction

We now move to explain the empirical formulas for extrapolating S-values of intrinsic cross-section terms of two-body and multi-body strong interaction in fusion reaction process.

Basic measure pion exchange force (PEF) is defined as the scale of effective surface area for very short range attractive force, that is the catch-ball of charged pion between neutron–nucleon and proton–nucleon between two fusing nuclei. One PEF is defined as the number of string between n and p, as illustrated in upper figure of Fig. 14.

As discussed in Section 1, sticking force of fusion happens at near surface of fusing nuclei.

The larger is the sticking surface area, the larger is the fusion cross-section. Using the PEF measure, PEF = 1 for HD fusion, PEF = 2 for DD fusion, and PEF = 3 for DT fusion, respectively, as example for DD fusion is drawn in the lower figure of Fig. 14.

Let us consider fusion reaction of deuteron with heavier nucleus, for example ^{6}Li + d fusion. As drawn by the right figure of Fig. 15, catch-ball of charged pions is interfered for about half of nucleons in ^{6}Li nucleus due to self-shielding by more front nucleons. As consequence of the self-shielding effect, PEF value would be around 3. For more heavy nuclei, PEF value should saturate to effective PEF values for interacting surface area.

On the contrary, multi-body deuteron fusion under the Platonic polyhedral configuration (e.g., regular tetrahedron for 4d fusion), there is no self-shielding effect. We can expect perfect exchange of charged pions among all deuterons of regular tetrahedral configuration as drawn in the left figure of Fig. 15. Thus, PEF = 12 is given for 4d fusion. Similarly PEF = 6 is given, for 3d fusion. We can say that effective sticking surface for multi-body fusion becomes very large as scaled by PEF number.

Table 4. All possible decay channels from ^{8}Be*

Decay-channel of ^{8}Be
4D → ^{8}Be + 47.6 MeV:
^{8}Be → ^{4}He + ^{4}He + 91.86 keV: Major Ch.
→ ^{3}He + ^{5}He(n + ^{4}He) − 11.13 MeV
→ t + ^{5}Li(p + ^{4}He) − 21.68 MeV
→ d + ^{6}Li − 22.28 MeV
→ p + ^{7}Li − 17.26 MeV
→ n + ^{7}Be − 18.90 MeV

^{8}Be excited state may open to threshold reactions

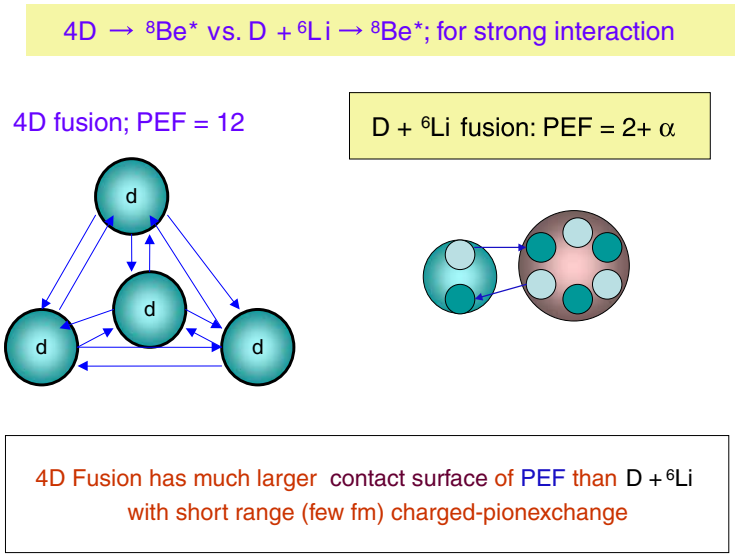

Figure 15. Estimation of effective sticking surface for fusion reactions, by the PEF measure for strength of charged pion exchange.

Here we recognize that ^{8}Be* is intermediate compound state both for the ^{6}Li + d and 4d reactions. And 4d fusion due to Platonic symmetry will have much larger cross-section than the ^{6}Li + d reaction.

Pion exchange force values, hence fusion cross-sections for 6d and 8d fusions in OSC condition may become much larger than 4d fusion.

Using known experimental $S(0)$-values for boson-related fusions, as pd, dd, and dt fusion, we draw plot of $S(0)$ values as a function of PEF value, and extrapolate to multi-body fusion using scaling formula, as shown in Fig. 16.

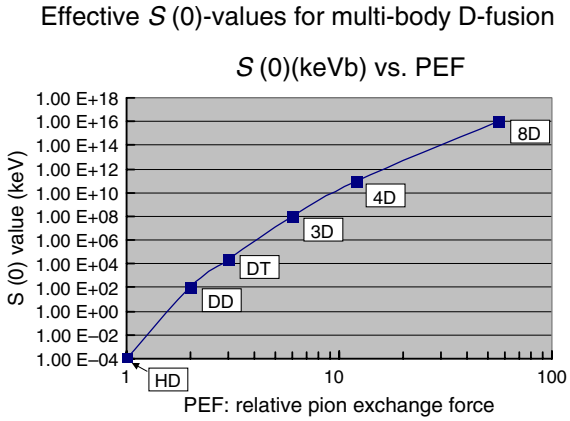

Figure 16. Empirical extrapolation of $S(0)$ values as a function of PEF (effective sticking surface of fusion reaction) number, for multi-body fusion.

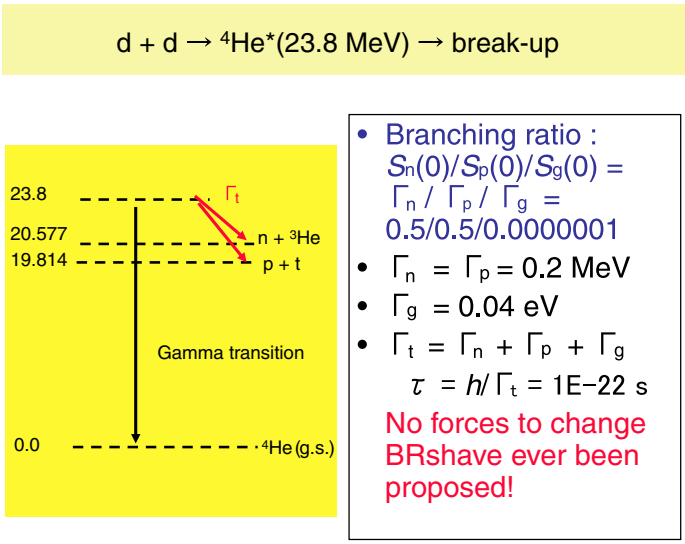

Figure 17. Final state interaction and branching ratios for dd fusion.

See also Fig. 2.

$$S_n(0) \propto T_n{}^2 \propto (\mathrm{PEF})^N. \tag{46}$$

Using $S_{dd} = 100$ keVb and $S_{dt} = 2 \times 10^4$ keVb, we estimated as scaling exponent $N = 11.4$ and we got $S_{4d} = 1 \times 10^{11}$ keVb.

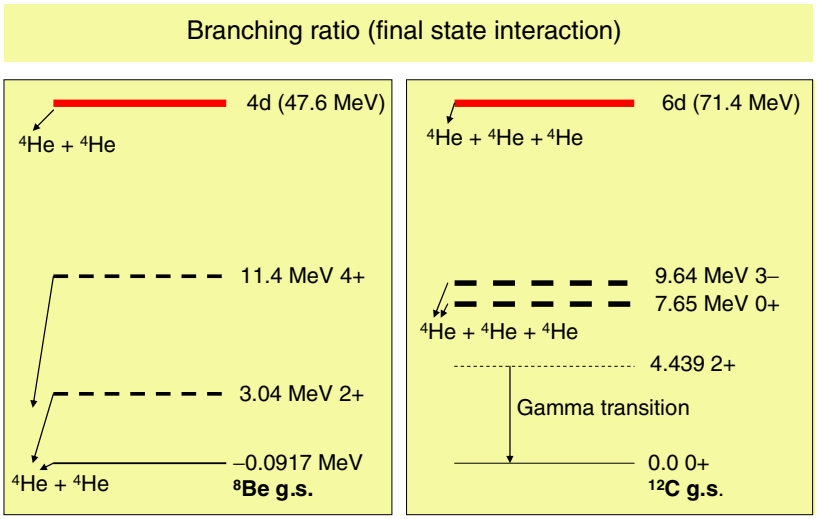

Figure 18. Final state interactions for 4d and 6d fusion reactions in condensed matter.

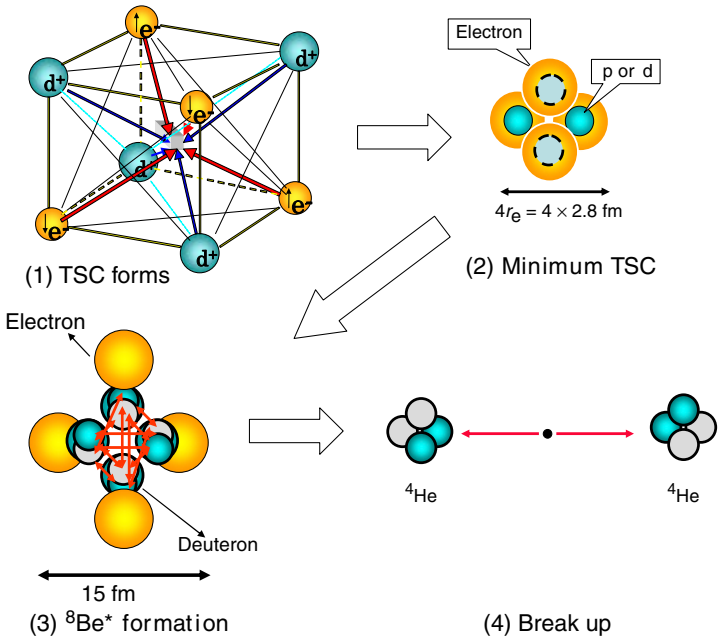

Figure 19. Semi-classical view of TSC squeezing motion and self-4d fusion reaction, here electron with spin should be electron-ball of 1/2 of two bosonized electrons in QM view.

Now we have finished preparation for fusion rate calculation. Calculated barrier penetration probabilities and fusion rates are shown in Table 3 for dde* EQPET molecules.

2.4. Final State Interaction

We now briefly summarize on the final state interactions and branching ratios to plural out-going channels.

The out-going break-up channels and branching ratios for dd fusion are very well established as shown in Fig. 17.

Unless we could change the intermediate excited state ^{4}He*($E_x = 23.8$ MeV) by some external forces putting in (see the lower figure of Fig. 14, for d–d reaction), we have no way to change the branching ratios. Namely, major channel for ^{4}He generation never happens otherwise. The electromagnetic interaction (QED, phonon coupling, etc.) is too weak to change the intermediate compound state. In the view of author, to put additional charged pion exchange into

Table 5. Time-averaged fusion rates by TDEQPET model, compared with values at $t = 0$

e*(m, Z)	$\langle\lambda_{2d}\rangle$ (f/s/cl.)	$\langle\lambda_{4d}\rangle$ (f/s/cl.)	$\lambda_{2d}(0)$ (f/s/cl.)	$\lambda_{4d}(0)$ (f/s/cl.)
TDEQPET cal. for EQPET molecules				
(1,1)	4.3×10^{-44}	7.8×10^{-63}	1.9×10^{-60}	7.3×10^{-93}
(2,2)	2.9×10^{-25}	2.5×10^{-24}	2.4×10^{-37}	1.1×10^{-50}
(4,4)	(2.1×10^{-17})*	5.5×10^{-8}	(5.5×10^{-22})*	5.9×10^{-20}

( )*: virtual value

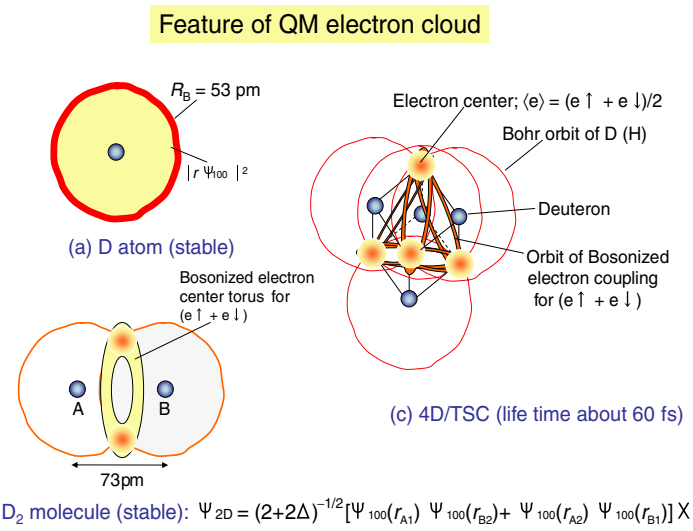

Figure 20. Initial state TSC wave function, compared with wave functions of D atom and D_2 molecule.

the d–d interaction by participating additional hadrons is actually possible way to get to the ^{4}He production: however, this idea leads ones automatically to the multi-body (or cluster) fusion process.

In Fig. 18, the final state interaction is drawn. The table of possible out-going channels is given in Table 4. The highly excited state ^{8}Be* can be regarded as a collectively deformed nucleus of two α-clusters, because of very hard formation of α-cluster in ^{8}Be nucleus. The very high (47.6 MeV) excited energy is therefore rarely redistributed to single nucleon (n or p), or d, or t-cluster for particle emission. Here one remembers that binding energy per nucleon for ^{4}He nucleus is 7 MeV and so total binding energy of ^{4}He nucleus is 28 MeV. This is the reason that α-cluster formation in light nuclei is very plausible.

We can speculate that all threshold reactions in Table 4 will not open in the final state interaction from 4d fusion, due to collective deformation of two α-clusters. Therefore, ^{8}Be* will decay with almost 100% weight to two ^{4}He with 23.8 MeV kinetic energy per ^{4}He, as illustrated in Fig. 18. The decay channel of 6d fusion by OSC is also shown in the right figure of Fig. 18. This process will give also 23.8 MeV per ^{4}He.

We know that p + ^{7}Li and n + ^{7}Be channels appear in the ^{6}Li + d beam-target reaction.

We understand that these branches are caused by stripping reactions taking n or p from deuteron approaching to ^{6}Li nucleus. The purely symmetric strong force exchange in the Platonic polyhedral condition, e.g., in the case of 4d/TSC reaction in PdD lattice, ignores the stripping process.

2.5. Time-dependent Approach

Detail of time-dependent analysis is given in Ref. [19]. Brief feature is illustrated in Fig. 19. The semi-classical squeezing motion of TSC will get to its minimum size state with about 10 fm diameter in about 74 fs. Calculated effective time-interval for 4d fusion is about 0.04 fs, namely very much short.

The TSC wave function at the starting point ($t = 0$) can be drawn by superposition of six D_2 molecule wave functions on six surfaces of cube, as shown in Fig. 20c. To calculate approximately time-dependent fusion rates, we

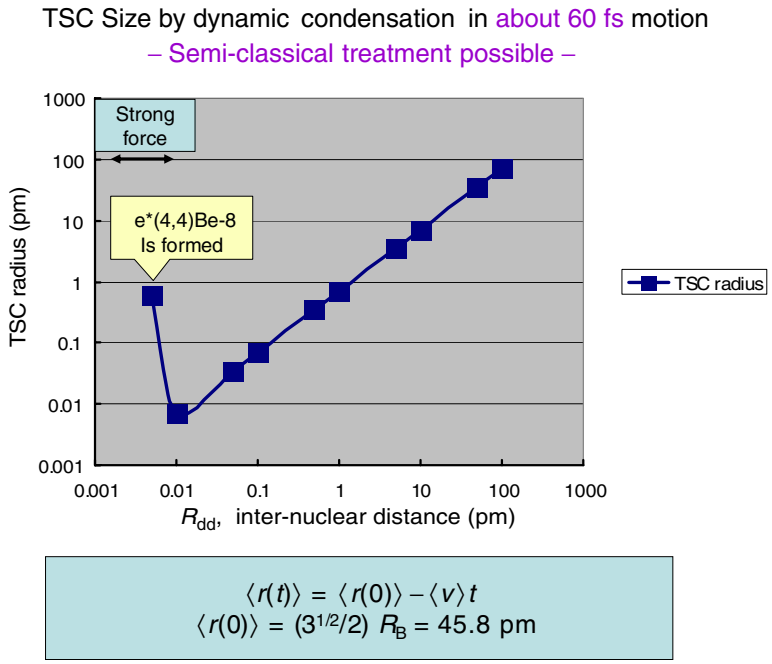

Figure 21. Linear decrease of TSC size by semi-classical Newtonian motion.

can use adiabatic dde* potentials, dividing into three time intervals for; normal electron state, Cooper pair state and quadruplet state, respectively. For more accurate analysis, we need to develop an algorithm of molecular dynamics under three-dimensional constraint motion. This is our future task.

Time-dependent squeezing motion of TSC was first treated by the time-dependent EQPET (TDEQPET) model [18].

$$a_i \Psi_{4D}(r,t) = a_1 \Psi_{(1,1)}(r,t) + a_2 \Psi_{(2,2)}(r,t) + a_4 \Psi_{(4,4)}(r,t), \tag{47}$$

$$\langle r(t)\rangle = \langle r(0)\rangle - \langle v\rangle t. \tag{48}$$

Because of the three-dimensionally and symmetrically constraint motion with averaged charge-neutrality for total TSC system, there is no force to stop squeezing motion until TSC size gets into the range of strong interaction (range of pion exchange). Therefore, the squeezing motion can be treated by the semi-classical Newtonian motion, as illustrated in Fig. 21.

To calculate time-dependent barrier penetration probability, we assumed that time-dependent change of potential can be replaced with three adiabatic potential V_s for D_2 molecule, dde*(2,2) and dde*(4,4) in three time intervals sequentially, according to the change of $\langle r\rangle$ value comparing with b_0-parameters of adiabatic potentials.

Time-dependent Gamow integral is defined as

$$\Gamma(t) = 0.218 \int_{r_0}^{b(t)} \sqrt{V_s(R_{dd}) - E_d}\ \mathrm{d}R_{dd}. \tag{49}$$

Here $b(t)$ is set to $\langle r(t)\rangle$ for $\langle r(t)\rangle > b_0$ parameter in each time interval for assumed adiabatic potential, namely e* state.

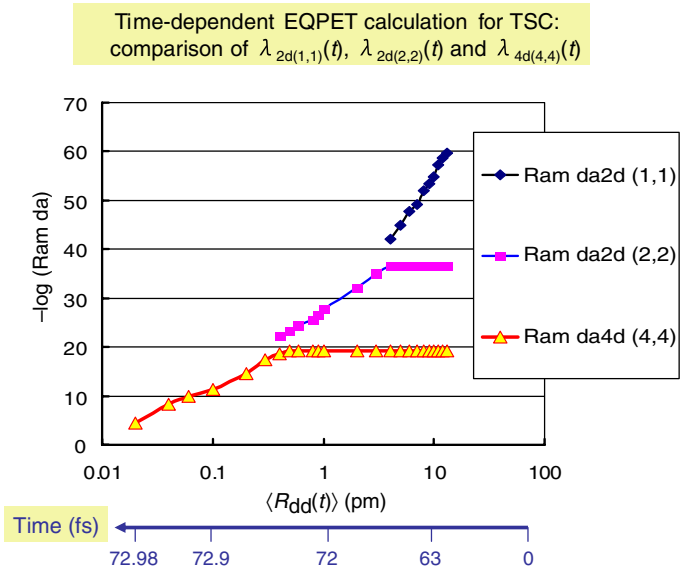

Figure 22. Calculated time-dependent fusion rates by TDEQPET model.

Time dependent fusion rates were calculated, as shown in Fig. 22. Time-averaged fusion rates were obtained as listed in Table 5.

Maximum TSC density possibly produced in PdD lattice is on the order of 1×10^{22} TSC/cm^3. Multiplying this number to cluster fusion rates in Table 5, we obtain dd fusion rate, which emit neutrons on the order of 3×10^{-3} n/s/cm^3. This level of neutron emission is difficult to detect by usual detectors. On the contrast, we obtain 4d fusion rate as $5.5 \times 10^{14} \alpha$ /s/cm^3 which corresponds to 55 kW/cm^3 power level. Thus, neutron free clean fusion reaction producing large heat density and ^{4}He ash, as reported by experiments of Arata, McKubre, de Ninno, Violante, Isobe, etc. can be now theoretically explained.

References

[1] J.M. Blatt, V.F. Weisskopf, *Theoretical Nuclear Physics*, Chapter VIII (Springer, Berlin, Heidelberg, New York, 1979).
[2] A. Takahshi et al., *JJAP* **41** (2001) 7031–7046.
[3] M. Ohta, A. Takahashi, *JJAP* **42** (2002) 645–649.
[4] A. Takahashi, Theoretical backgrounds for transmutation reactions, ppt slides for Sunday School of ICCF10, see http://www.lenr-canr.org/ Special Collection for ICCF10.
[5] B. Povh, K. Rith, C. Scholtz, F. Zetsche, *Teilchen und Kerne* (Springer, Berlin, Heidelberg, New York, 1994).
[6] K. Yagi, *Nuclear Physics* (Asakura, Tokyo, 1971) (in Japanese).
[7] L.I. Schiff, *Quantum Mechanics* (McGraw-Hill, New York, 1955).
[8] P.M. Morse, H. Feshbach, *Methods of Theoretical Physics* (McGraw-Hill, New York, 1953).
[9] X.Z. Li et al., *Phys. Rev. C* **61** (2000) 24610.
[10] A. Takahashi, Condensed matter nuclear effects, *Proceedings of the. International Meet. Frontiers of Physics*, Kuala Lumpur, 25–29 July, 2005, *Malays. J. Phys.* to be published.

[11] A. Takahashi, Deuteron cluster fusion and related nuclear reactions in metal-deuterium/hydrogen systems, *Recent Res. Dev. Phys.* **6** (2005) 1–28, ISBN: 81-7895-171-1.
[12] A. Takahashi, *Proceedings of the ICCF9*, pp. 343–348, see Ref [2].
[13] A. Takahashi, Mechanism of deuteron cluster fusion by EQPET model, *Proceedings of the ICCF10*, see Ref [3].
[14] A. Takahashi, *Proceedings of the JCF5, 6*, see http://wwwcf.elc.iwate-u.ac.jp/jcf/.
[15] A. Takahashi, *Proceedings of the ICCF11*.
[16] A. Takahashi, Deuteron cluster fusion and ash, *Proceedings of the ASTI5 Meeting*, see Ref [5].
[17] A. Takahashi, A theoretical summary of condensed matter nuclear effects, in: A. Takahashi (Ed.), *Proceedings of the Siena2005 Workshop*, see also: *Brief Theoretical Summary of Condensed Matter Nuclear Effects*, Debrecen, Hungary, 2005, *Acta Phys. et Chem.* **38–39**, 341–356.
[18] A. Takahashi, Time-dependent EQPET analysis of TSC, *Proceedings of the ICCF12*, Yokohama, 2005.
[19] C.J. Pethic, H. Smith, *Bose-Einstein Condensation in Dilute Gases* (University of Chicago Publication, Chicago, 2001).
[20] A. Takahashi, H. Numata, Y. Iwamura, H. Yamada, T. Ohmori, T. Mizuno, T. Akimoto, *Nuclear Reactions in Solids* (Kogakusha, Tokyo, 1999) (in Japanese).
[21] S. Shirato, *Atomic Physics-II* (Nippon Rikou Publ., Tokyo, 1984) (in Japanese).